Amalgamation of Solid Dispersion and Melt Adsorption Techniques For Augmentation of Oral Bioavailability of Novel Anticoagulant Rivaroxaban

Pranav Shah (pranav.shah@utu.ac.in)
Maliba Pharmacy College
Milan Patel
Maliba Pharmacy College
Jigar Shah
Nirma University Institute of Pharmacy
Anroop Nair
King Faisal University
Sabna Kotta
King Abdulaziz University
Bhavin Vyas
Maliba Pharmacy College

Research Article

Keywords: Rivaroxaban, solid dispersion adsorbate, dissolution, factorial design, pharmacokinetics, pharmacodynamics

Posted Date: November 12th, 2021

DOI: https://doi.org/10.21203/rs.3.rs-997661/v1

Abstract

The objective of the present study was to evaluate the potential of solid dispersion adsorbate to improve the solubility and bioavailability of rivaroxaban (RXN). Solid dispersion adsorbate (SDA) of RXN was developed by fusion method using PEG 4000 as carrier and Neusilin as adsorbent. A 3^2 full factorial design was utilized to formulate various SDAs. The selected independent variables were amount of carrier (X_1) and amount of adsorbate (X_2). The responses measured were time required for 85% drug release (Y_1) and saturated solubility (Y_2). MTT assay was employed for cytotoxicity studies on Caco-2 cells. *In vivo* pharmacokinetics and pharmacodynamic evaluations were carried out to assess the prepared SDA. Pre-compression evaluation of SDA suggests the prepared batches (B1-B9) possess adequate flow properties and could be used for compression of tablets. Differential scanning calorimetry and X-ray diffraction data signified the conversion of crystalline form of drug to amorphous form, a key parameter accountable for improvement in drug dissolution. Optimization data suggests that the amount of carrier and amount of adsorbate significantly ($P < 0.05$) influence both dependent variables (time required for 85% drug release and saturated solubility). Post-compression data signifies that the compressibility behavior of prepared tablets were within the official standard limits. Significant increase ($P < 0.0001$) in the *in vitro* dissolution characteristics of RXN was noticed in optimized SDA (>85% in 10 min) as compared to pure drug, marketed product and directly compressible tablet. Cytotoxicity studies confirm nontoxicity of prepared RXN SDA tablets. Higher C_{max} and AUC achieved with RXN SDA tablets indicated enhancement in oral bioavailability (~3 folds higher than the RXN suspension). Higher bleeding time and percentage of platelet aggregation noticed with RXN SDA tablets further substantiate the efficacy of the prepared formulation. In summary, the results showed the potential of RXN SDA tablets to enhance the bioavailability of RXN and hence can be an alternate approach of solid dosage form for its development for commercial application.

Introduction

Chemically Rivaroxaban (RXN) is 5-Chloro-N-([(5S)-2-oxo-3-[4-(3-oxo-4morpholinyl) phenyl]-1, 3 oxazolidin-5-yl] methyl)-2-thiophene-carboxamide. It can directly inhibit activated serine protease Factor Xa (FXa), when given orally as monotherapy for treating venous thromboembolism. It is the first reported potent orally active anticoagulant widely used for the prophylaxis of deep vein thrombosis. The conventional anticoagulants like vitamin K, heparin etc. suffer from toxic effects and low efficiency and hence fail to produce a satisfactory outcome (1). RXN competitively inhibits FXa, which is required for the activation of prothrombin to thrombin. Selective binding of this drug stops thrombin formation and clotting. Unlike conventional anticoagulants, which may cause profuse internal bleeding, disability or brain death, RXN does not require therapeutic drug monitoring and therefore considered to be safe. Since RXN can avoid major bleeding, it was proved to be superior in clinical medicine than warfarin in the management of embolism and stroke (2). However, its low aqueous solubility indirectly results in a difference between fasted and fed state drug absorption. It is non-ionizable and insoluble in water (5-7 mg/l at 25°C) with high lipophilicity and thus falls in BCS class II (3).

Numerous novel formulation strategies have been utilized to enhance the aqueous solubility of BCS class II drugs, like liposomes, cyclodextrin inclusion complexes, use of cosolvents, nanoemulsion, nanosuspensions, solid dispersions etc. (4–8). Various studies have been done for enhancing the solubility, dissolution characteristics and bioavailability of RXN including inclusion complexes (9), self-nanoemulsifying drug delivery systems (SNEDDS) (1, 3), nanoparticles (2) and microparticles (10). However, these formulation strategies are not devoid of limitations and scaling up in industries is a major challenge.

Solid dispersion consists of a minimum of two different components, usually a hydrophilic inert carrier/ matrix and a lipophilic drug. The carrier may be amorphous or crystalline in nature. Typically, it is a dispersion of an active ingredient in a matrix or in an inert carrier formulated by melting, using solvent, or melting solvent method. In this system, the drug experiences particle size reduction and as a result dissolution is increased due to increase in surface area. Additionally, no energy is needed to break the crystal-lattice of the drug in the amorphous state throughout the dissolution step (11). Due to the presence of surrounding hydrophilic carriers, drug wettability as well as solubility will be increased further (12). Attempts were also made to formulate solid dispersions of RXN to enhance the drug dissolution, solubility and thereby enhance the absorption (13–15). However, there are some limitations for this technique as well, which includes, difficulty in grinding, inadequate flow, poor compressibility, and also less reproducibility of physicochemical properties, instability of the drug and vehicle as well as difficulty in scale-up (5, 16). The concept of solid dispersion adsorbate (SDA) was introduced to control these problems. In this method solid dispersion is adsorbed on a carrier with very large surface area to obtain a freely flowing powder and thereby help in increase in dissolution as well as bioavailability (17–19). There are a variety of commercially available porous carriers like Florite, Neusilin US2, Aerosil, Aerogel etc. having unique characteristics like pore size, particle size, specific surface area etc. and has been widely investigated in tablet formulations (20–22). In this study, Neusilin US2 was used as the adsorbent. Neusilin US2 is amorphous aluminium magnesium silicate with a high level of specific surface area and good adsorption capacity. On the other hand, polyethylene glycol (PEG) has been widely used in various oral formulations including tablets, microcapsules, soft gelatin capsules, suspensions and emulsions (23). Indeed, the PEG 4000 (hydrophilic polymer) is one of the most widely studied polymeric carriers in preparing solid dispersion (24–26), and is used as a carrier in the present study. Thus the objective of this study was to formulate SDAs of a model drug-RXN by amalgamation of solid dispersion and melt adsorption techniques and assess its potential to improve the solubility and dissolution. However, a review of literature suggests that no work has been done on RXN SDA for solubility enhancement. A 2-factor, 3-level experimental design was utilized to statistically optimize various formulation components and assess main effects. The effects of independent variables (amount of carrier- PEG 4000 and adsorbate- Neusilin US2) on the dependent variables (time required for 85% drug release and saturated solubility) were assessed. The prepared SDA batches (B1-B9) were assessed for both pre and post compression properties. Optimized RXN SDA was evaluated for cytotoxicity, pharmacokinetics and pharmacodynamics properties.

Experimental Methods

Materials

RXN was obtained from Symed Labs limited, Hyderabad, India. Neusilin US2 was obtained from Gangwal Chemicals Pvt. Ltd., Mumbai, India. Micro crystalline cellulose (PH 102) was purchased from Signet, Mumbai, India. Polyethylene glycol (PEG) 4000, crospovidone, magnesium stearate, and talc were acquired from S.D. Fine Chem. Products, Mumbai, India. The cell lines of human colorectal adenocarcinoma (Caco-2) were procured from the National Center for Cell Science, Pune, India. Culturing of cells were performed in Dulbecco's Modified Eagle's medium (Sigma-Aldrich, USA) supplemented with 10% fetal bovine serum, 100 IU/mL penicillin, 100 µg/mL streptomycin, 1% non-essential amino acids in a humidified environment of 5% CO_2 using a carbon dioxide incubator (Thermo Scientific, Waltham, MA, USA) at 37°C. All other chemicals were of analytical grade.

Preparation of SDA

SDA of RXN was prepared by a fusion method reported in literature (17) with minor modifications. In this method the RXN and PEG 4000 were taken in the molar ratio and Neusilin US2 as an adsorbent. The carrier (PEG 4000) was melted in the porcelain dish and heated further till its melting point (57-63°C) on a hot plate. Then, RXN (0.435 g) was dispersed into melted carrier mass with constant stirring to form solid dispersion. Further, the adsorbate (Neusilin US2) is added and stirred until the blend is converted into a free-flowing powder. The SDA was then passed through number 40 mesh sieve.

Experimental Design (QBD-DOE Approach)

A 2-factor, 3-level full factorial experimental design was chosen to optimize various formulation parameters statistically and the effects of various formulation components on solubility and *in vitro* release of formulations was evaluated. The selected dependent and independent variables are presented in Table 1 along with their low (-1), medium (0) and high (+1) levels. The amount of carrier and adsorbate was selected from the results of preliminary experiments and previous literature (27, 28). An experimental design comprising of 9 design batches was developed with different amounts of carrier (X_1) and amount of adsorbate (X_2) Coded and non-coded values of design batches are shown in Table 2.

Table 1
Independent and dependent variables used for experimental design

Independent variables	Levels		
	Low (-1)	Medium (0)	High (+1)
Amount of carrier; PEG 4000 (g) =X_1	4	6	8
Amount of adsorbate; Neusilin US2 (g) =X_2	0	1.5	3
Dependent variables			
$Y_1 = t_{85\%}$ (time required for 85% drug release)			
Y_2 = Saturated solubility			

Table 2
Formulation of solid dispersion adsorbate batches

Batch No.	X_1	X_2	Polyethylene glycol 4000 (g)	Neusilin US2 (g)
B1	-1	-1	4	0
B2	-1	0	4	1.5
B3	-1	+1	4	3
B4	0	-1	6	0
B5	0	0	6	1.5
B6	0	+1	6	3
B7	+1	-1	8	0
B8	+1	0	8	1.5
B9	+1	+1	8	3

Percentage Yield and Solubility

Percentage practical yield of the prepared SDA batches (B1-B9) was calculated for determining the productivity of the formulation technique. The practical yield was determined by the equation; % Practical yield = (Weight of prepared SDA/Theoretical weight of SDA) x100.

The solubility of the RXN in prepared SDA batches (B1-B9) was setimated by adding an excess amount of drug containing SDAs in 10 mL distilled water in glass vials (29). The mixture was mixed in a thermomixer C (MixMate, Eppendorf, Germany). The shaking of the mixture continued for 24 h at 25°C. The solution was then sonicated for 20 min and supernatant was taken and passed through syringe filter (0.45 µm). The filtrate was diluted and the absorbance was recorded on UV spectrophotometer (UV Shimadzu 1800 Scientific Instrument, Japan) at λmax of 248 nm.

Evaluation of Flow Characteristics of SDA

The characteristics like angle of repose, bulk density, tapped density, Carr's index and Hausner's ratio of prepared SDA were measured as pre-compression evaluation by standard protocols (30, 31).

Characterization of SDA

FTIR Spectroscopy

The IR peaks of optimized SDA, RXN and Neusilin US2 were characterized by FTIR spectroscopy (Bruker Optics GmbH, Ettlingen, Germany). RXN and potassium bromide were mixed and made into pellets by compressing the powder mixture on potassium bromide press at 20 psi for 10 min (32). The spectrum was taken from the range of 4000 to 400 cm^{-1} (Wavenumber).

X-ray Powder Diffraction (XRD)

Diffractograms of RXN, Neusilin US2 and SDA were recorded using a diffractometer (Rigaku Corporation-Miniflex, Surat, India). The samples were finely ground in a mortar with the help of a pestle and samples were irradiated with X-ray at scanning angle in the range of 0° to 40° of 2θ.

Differential Scanning Calorimetry (DSC)

DSC thermograms of RXN, Nesulin US2 and SDA were characterized by DSC (DSC-60, Shimadzu Corporation, Kyoto, Japan). Thermal performance of the samples was studied by keeping (3-5 mg) in an aluminium pan and sealing hermetically, while a blank pan was used as standard reference (33). Thermal behaviour was determined at a scanning speed of 10°C/min at temperature between 25–300°C under nitrogen atmosphere (10 mL/min).

Surface Morphology

Morphological examination of prepared SDA was carried out by scanning electron microscopy (Hitachi S-3400, India) operated at specific voltage of 15 kV. Samples were mounted on metal stubs and were made conductive by coating with platinum in neutral condition while maintaining the pressure (34). Then the images were captured using a microscope.

Formulation of SDA Tablets

The SDA was weighed accurately to obtain a weight of 10 mg of drug. Micro crystalline cellulose and crospovidone were added into it and were mixed for 5 min. Then magnesium stearate and talc were added and again mixed for 2 min. The mixtures were passed through sieve no. 100 and compacted into tablets using 10 mm punch in tablet compression machine (Rimek mini press-I, Ahmedabad, India). Table 3 shows the composition of tablets prepared from SDA.

Table 3
Composition of immediate release SDA tablets

Batch No.	Solid dispersion adsorbate (mg)	Crospovidone (mg)	Micro crystalline cellulose (mg)	Talc (mg)	Magnesium stearate (mg)	Quantity per tablet (mg)
B1	101	15	179	2.5	2.5	300
B2	136	15	144	2.5	2.5	300
B3	170	15	110	2.5	2.5	300
B4	147	15	133	2.5	2.5	300
B5	182	15	98	2.5	2.5	300
B6	216	15	64	2.5	2.5	300
B7	193	15	87	2.5	2.5	300
B8	228	15	52	2.5	2.5	300
B9	262	15	18	2.5	2.5	300

Evaluation of SDA Tablets

The compressed tablets were characterized for general appearance, thickness, weight variation, hardness, friability, disintegration time and assay according to the standard protocols (35).

In vitro Dissolution

The dissolution profile of immediate release tablets prepared from the SDA batches (B1-B9) was done on USP type II apparatus (Electrolab TDT-08L, Mumbai, India) at 75 rpm. The dissolution medium used was acetate buffer (pH 4.5; 900 mL) containing 0.4% sodium dodecyl sulfate with temperature setting at 37 ± 0.5°C (36). Samples (10 mL) were taken out for analysis at different time points (5, 10, 15, 20, 25, 30, 40, 50 and 60 min). The sample was analyzed at 248 nm using UV spectroscopy after filtering through Millipore filter (0.45 µm; Spectrum Medical Inc., San Diego, CA). Using the calibration curve equation, the cumulative percentage of RXN release at various time intervals was calculated. Similarly, *in vitro* drug release of optimized SDA tablet was performed and the profiles were compared with pure drug, marketed product and directly compressible tablet.

Cytotoxicity Test

The cytotoxicity of prepared RXN SDA tablets and suspension containing RXN against the Caco-2 cell line was determined by MTT assay. In brief, cells were seeded at a density of 7.5×10^4 cells/mL (200 µL/well) in 96-well culture plates and incubated with 20-100 µM of RXN SDA tablets or RXN suspension. After 24 h of incubation, the MTT reagent (25 µL; 5 mg/mL in PBS, 25 µL/well) was poured to individual well and kept at 37°C for 4 h, in order to metabolize MTT. The formed formazan precipitate was dissolved by

adding DMSO (100 µL) to every well. The optical density of the samples was determined at 570 nm with the help of a plate reader (Bio-Rad, iMark, Hercules, CA, USA) and background was deducted at 630 nm. The estimation of percent cell viability was made based on the formula described in the literature (37).

Pharmacokinetic Study

A total of 12 male Sprague-Dawley rats were included in the study. The animals were randomly divided into two groups. Group I, and Group II were administered RXN suspension, and RXN SDA tablets, respectively (equivalent to 10 mg/kg of RXN) (38). RXN SDA tablets was powdered and dispersed in 0.5% w/v carboxymethyl cellulose (39). Pharmacokinetic study was performed in Maliba Pharmacy College, Uka Tarsadia University, as per the animal ethics committee approved protocol MPC/IAEC/21/2017 and CPCSEA guidelines. Each group was administered 0.5 mL of sample by oral route. At particular time intervals (0, 0.25, 0.5, 1, 2, 3, 4, 8, 12, and 24 h), 200 µL blood was collected from the post-orbital plexus. Blood samples were centrifuged for 5 min at 4°C in a cooling centrifuge at 16,000 x g, and the supernatant plasma was collected. WinNonlin software 8.1 (Pharsight, Sunnyvale, CA, USA) was employed to perform non-compartmental pharmacokinetic analysis. From the plot of drug plasma level vs. time, pharmacokinetic parameters, namely maximum plasma concentration of RXN (Cmax) and the time required to achieve the maximum plasma concentration of RXN (Tmax) were calculated. The area under the curve (AUC) was determined using the trapezoidal law from 0 to 24 hours (AUC0–24), and by extrapolating the time to infinity was used to calculate the AUC of the profile from 0 to infinite time (AUC0–∞).

Pharmacodynamic Studies: Pharmacodynamic studies were performed in Maliba Pharmacy College, Uka Tarsadia University, as per the animal ethics committee approved protocol MPC/IAEC/21/2017 and CPCSEA guidelines.

Tail Bleeding Time Assay

Animals were divided into three groups comprising 6 rats per group, to estimate tail bleeding duration. Group I received 0.5% w/v carboxymethyl cellulose (control); Group II received RXN suspension and Group III received RXN SDA tablets dispersed in 0.5% carboxymethyl cellulose. Groups II and III received doses equivalent to 10 mg/kg of RXN. All treatments were given orally once. Four hours post-administration; animals were anesthetized by administering pentobarbital sodium (50 mg/kg intraperitoneal) (40). The method of Wang et al. (2004) with slight modifications was adopted to determine the rat tail bleeding time (41). A 5 mm rat tail tip was amputated with a scalpel to determine the bleeding time, and blood was blotted onto filter paper every 30 seconds before the staining of the paper with blood ceased. The bleeding time was described as the time between the amputation of the tail and the cessation of bleeding (min).

Platelet Aggregation

This study was performed in rats for all three groups after tail bleeding time assay. Blood was spontaneously withdrawn from the abdominal aorta and collected in the vial containing anticoagulant,

acid-citrate-dextrose (9:1, v/v containing citric acid 130 mM, trisodium citrate 170 mM, dextrose 4%). The platelets were prepared according to the process mentioned previously (42). Briefly, platelet-rich plasma was collected by centrifuging blood at 3600 rpm for 15 min. *In vitro* platelet aggregation was evaluated according to the method of Born (43). Platelet aggregation was performed using an aggregometer at 37ºC and 1000 rpm. The 240 µL of washed platelets were stimulated with an aggregating agent i.e., collagen (5 mg/mL). Platelet aggregation was registered for a 10 min period after platelet stimulation.

Data Analysis

The statistical interpretation of experimental data was carried out with GraphPad Prism (version 6, GraphPad, San Diego, CA, USA). The difference in values at $p < 0.05$ is considered statistically significant.

Results And Discussion

Percentage Yield and Saturated Solubility

Prepared batches (B1-B9) were evaluated for percentage yield and saturated solubility and the data are summarized in Table 4. The percentage yield was found to be more than 90% in all batches (Table 4) and was highest with B9. On the other hand, the saturated solubility of RXN significantly improved with the addition of carriers (PEG 4000 and Neusilin US2), and also showed improvement with increase in carrier content. The highest RXN solubility noticed was 0.041 mg/mL, which is 3.4 times higher as compared to solubility of pure drug in water (0.012 mg/mL). This improvement in solubility of RXN could be due to the potential of hydrophilic PEG 4000 (carrier) to improve the wettability of the drug (44) as well as the Neusilin US2 (adsorbate), which increases the surface area of the formulation (45, 46).

Table 4
Percentage yield and saturation solubility of different solid dispersion adsorbate batches

Batch No.	% Yield	Solubility (mg/mL)
B1	95.83±1.02	0.026±0.005
B2	96.03±1.68	0.029±0.001
B3	95.84±0.86	0.038±0.006
B4	95.84±0.23	0.027±0.006
B5	97.45±1.45	0.038±0.003
B6	96.90±0.54	0.041±0.007
B7	96.83±0.49	0.023±0.001
B8	97.54±1.05	0.028±0.004
B9	98.23±0.36	0.031±0.002

Flow Characteristics of SDA

The results of angle of repose, bulk density, tapped density, Carr's index and Hausner's ratio of different batches of SDA are presented in Table 5. The data here signifies all the prepared batches possess adequate flow properties and could be used for compression of tablets.

Table 5
Flow characteristics of different solid dispersion adsorbate batches

Batch No.	Angle of repose (°)	Bulk density (g/cm^3)	Tapped density (g/cm^3)	Carr's index (%)	Hausner's ratio
B1	27.78±0.16	0.68±0.05	0.79±0.07	13.85±1.03	1.15±0.01
B2	21.64±0.11	0.43±0.02	0.53±0.03	18.12±0.10	1.21±0.01
B3	17.25±0.29	0.42±0.02	0.46±0.03	9.25±0.65	1.09±0.01
B4	20.92±0.11	0.53±0.03	0.59±0.04	10.82±0.80	1.11±0.01
B5	20.41±0.21	0.46±0.03	0.51±0.03	9.96±0.58	1.10±0.01
B6	17.73±0.31	0.43±0.02	0.51±0.05	9.62±0.65	1.17±0.08
B7	22.07±0.24	0.79±0.07	0.94±0.09	16.15±1.47	1.18±0.02
B8	21.40±0.18	0.57±0.04	0.75±0.07	22.78±0.44	1.22±0.11
B9	18.10±0.14	0.43±0.02	0.50±0.05	9.62±0.64	1.11±0.07

Characterization of SDA

FTIR

The FTIR spectra of pure RXN, PEG 4000, Neusilin US and SDA are presented in Figure 1. The prominent peaks of various functional group of RXN were observed at 3351 cm^{-1} (N-H stretch), 1736 cm^{-1} (C=O stretch carbonyl group), 1646 cm^{-1} (C=O stretch ester group), 1516 cm^{-1} (N-O stretch), 828 cm^{-1} (Benzene stretch). From the figure, it is observed that the infrared spectrum of pure drug and SDA have significant difference in the absorption peaks intensity. A slight shift towards the lower wavelength or broadening was noticed in few peaks.

XRD

The diffraction spectra of RXN, PEG 4000, Neusilin US2 and solid dispersion of RXN adsorbate are shown in Figure 2. The graph of pure RXN showed high crystalline nature of the drug with main diffraction peaks. The X-ray diffractogram of SDA didn't show any characteristic peaks which are observed in pure drug diffraction patterns, which indicates transformation of crystalline to amorphous form of the drug. The possible reason for this change could be due to the annihilation of RXN crystal lattice, because of homogenous dispersion of drugs into molten carriers. Therefore, the reduction in crystallinity of the drug might be pertaining to improvement in dissolution of RXN.

DSC

The DSC thermogram of pure drug, Neusilin US2, PEG 4000 and SDA are presented in Figure 3. RXN showed a distinct strong endothermic peak at 230°C (which is the drug melting point), which indicates its crystalline nature. However, the DSC of SDA did not show any peak of pure RXN; this might be due to the complete dissolution of RXN in the melted polymer which indicated that the drug can be in an amorphous state.

SEM

SEM images were captured to observe the surface morphology of the SDA (Figure 4). The SEM of the RXN powder were found to be irregular in shape as well as exist as crystalline particles in the aggregates. It has been described that Neusilin US2 is porous in nature with numerous inter and intra particle apertures exists on its surface that can contribute enormous surface area and eventually helps in greater adsorption (47). Further, the SEM images in Figure 4 also demonstrated total adsorption of PEG 4000 and RXN on the surface of Neusilin US2. This observation confirms that the particles in the prepared SDA did not aggregate and possess free flowing properties.

Evaluation of SDA Tablets

Physical examination of tablets from each batch showed that all the tablets were circular, white to off white, flat and without any physical defects. The results of immediate release SDA tablets are shown in Table 6. Thickness of SDA tablets ranged from 3.10±0.02 to 3.48±0.02 mm while the diameter of tablets was found to be in the range of 8.10 ± 0.001 to 8.19 ± 0.001 mm, hence all tables are in the acceptable range. Similarly, all formulations showed uniformity of weight within the pharmacopoeia limits for uncoated tablets. Hardness of SDA tablets ranged from 2.41±0.20 to 2.83±0.28 kg/cm^2, which assures the tablets withstand during handling and transportation and also can bear the wear and tear. Friability was in the range of 0.32±0.02 to 0.48±0.05%, which ensures acceptable resistance by tablets to withstand mechanical shocks and can withstand wear and tear. Disintegration time was ranging between 25.33±0.57 to 44.23±1.52 sec. Batches B1, B4 and B7 which contain no adsorbate showed more disintegration time (44, 41 and 43 sec), rest of batches which contain adsorbate showed less disintegration time (Table 6). From the results it was clear that the presence of adsorbate in formulation decreases disintegration time due to increased surface area. The percentage drug content of all the batches of SDA were found to be between 96.15 – 99.60%, which are in acceptable range.

Table 6
Evaluation of physicochemical properties of immediate release SDA tablets

Batch No.	Average weight (mg)	Thickness (mm)	Hardness (kg/cm^2)	% Friability	Disintegration time (sec)	Drug content (%)
B1	302±4.02	3.10±0.02	2.83±0.28	0.48±0.05	44.23±1.52	101.12±1.62
B2	301±4.24	3.43±0.01	2.60±0.17	0.53±0.04	34.33±0.57	102.35±1.45
B3	301±4.10	3.33±0.01	2.50±0.26	0.58±0.01	26.00±2.64	100.52±1.04
B4	303±3.74	3.48±0.02	2.70±0.20	0.46±0.02	41.33±1.52	102.45±1.24
B5	302±3.19	3.31±0.01	2.55±0.14	0.40±0.01	29.33±2.08	104.12±0.65
B6	300±2.97	3.44±0.01	2.41±0.20	0.32±0.02	25.33±0.57	103.14±1.68
B7	303±3.27	3.19±0.01	2.73±0.12	0.45±0.03	43.66±2.08	104.68±0.63
B8	302±3.34	3.41±0.01	2.63±0.20	0.34±0.04	31.00±2.64	105.12±1.64
B9	300±2.70	3.14±0.01	2.56±0.21	0.32±0.02	27.66±0.57	104.26±1.38

In Vitro Dissolution

Drug release profile of all the SDA tablets was shown in Figure 5. The release patterns of all batches showed fast dissolution. Batches (B3, B5, B6, B8 and B9) exhibited more than 85% dissolution in 10 min. In all the batches concentration of carrier (X_1) and concentration of adsorbate (X_2) played an important role in drug dissolution rate. The pure drug showed weak dissolution rate ($p < 0.001$) due the absence of carrier and adsorbate and hence the low solubility of RXN in aqueous phase resulted in the slow release of the drug. Batches B1, B4, and B7 showed decrease in dissolution rate compared to other batches due the absence of adsorbate in those batches but they have more dissolution rate than pure drug, which confirmed the formation of solid dispersion. Batches B2, B5, B8, B10 and B11 showed increased percentage drug release due to the presence of adsorbate, which helped in increasing the surface area of formulation and thereby increasing dissolution. Batches B3, B6 and B9 showed increased percentage drug release due to the higher concentration of adsorbate in those batches. The enhancement in the dissolution of RXN from SDA tablets formulations can be ascribed due to several factors like enhanced surface area offered for drug release, improvement in aqueous solubility of the drug, and increased wettability of the drug particles. The immediate sinking of the particles was noted during the dissolution studies.

Fitting Data to the Model

A 2-factor, 3-level experimental design was utilized as the RSM needed 9 experiments. The responses observed with all the nine batches were concurrently fit to a quadratic model using design expert software version 11.0. The independent variables and response of dependent variables are shown in Table 7. The best fit model observed was the quadratic model. A positive number indicates an effect that favors the

optimization, on the other hand, a minus number suggests that the relation between factor and response is negative. It is evident that both the independent variables, viz., the amount of carrier (X_1) and the amount of adsorbate (X_2) have positive effects on the responses, viz., t85 (time required for 85% drug release) and saturated solubility.

Table 7
Design layouts with respective observed response

Batch No.	X_1 amount of carrier	X_2 amount of adsorbate	$Y_1 = t_{85}\%$ (min)	Y_2 =saturated solubility (mg/mL)
B1	-1	-1	16.10	0.026
B2	-1	0	15.20	0.029
B3	-1	+1	10.15	0.038
B4	0	-1	15.30	0.027
B5	0	0	9.40	0.038
B6	0	+1	9.10	0.041
B7	+1	-1	14.45	0.023
B8	+1	0	9.30	0.028
B9	+1	+1	8.55	0.031

Data Analysis of Y_1 (Time Required for 85% Drug Release)

The observed values of t_{85} for all the 9 batches varied from 8.55 to 16.10 min. The outcome certainly indicated that Y_1 is deeply affected by the amount of carrier and amount of adsorbate for study. The batch 9 showed the highest t_{85} and batch 1 gave the minimum t_{85}. The response (Y_1) obtained for two independent variables was exposed to multiple regression to get quadratic polynomial equation:

$$Y_1 \text{ (Full model)} = +10.62 - 1.53X_1 - 3.01X_2 + 0.0125X_1X_2 + 1.03X_1^2 + 0.975X_2^2$$

The above equation clearly illustrates the broad range of numbers for different coefficients. The coefficient value for independent variable X_1 (-1.53) signifies the positive response on the dependent variable Y_1, so increasing carrier amount led to decrease in time required for 85% drug release. This is due to the potential of hydrophilic PEG 4000 to improve the wettability of the drug as described in the literature (44). Similarly, the coefficient value for X_2 (-3.01) shows the positive response on drug release, i.e. on increasing adsorbate amount leads to decrease in the time required for 85% drug release. The possible explanation for this observation could be due to the potential of Neusilin US2 to enhance the dissolution rate by increasing the effective surface area (46) and/or conversion of crystalline RXN to amorphous state (48) and/or favored rapid diffusion of molecularly dispersed drug through the pores

(28). The regression coefficients having P value < 0.05 are considered as highly significant. The term X_2 with P value < 0.05 was significant in contributing to prediction of time required for 85% drug release. The reduced equation for RXN can now be written as:

Y_1 (Reduced model) =+10.62 -3.01X_2

The independent variable X_2 (amount of Neusilin US2) was found significant (P < 0.05) in affecting Y_1 ($t_{85\%}$). Figure 6a shows contour plot and 2b exhibits 3d surface response plot of time required for 85% drug release. It is clearly observed from the graphs that as the amount of carrier and amount of adsorbate increases, the time required for 85% drug release decreases.

Data Analysis of Y_2 (Saturated Solubility)

The observed values of saturated solubility for all 9 batches varied from 0.023- 0.041 mg/mL. The results clearly showed that Y_2 is also affected by the amount of carrier and amount of adsorbate in the study. Batch 6 showed highest solubility (0.041 mg/mL) and batch 7 gave minimum solubility (0.023 mg/mL). The response (Y_2) obtained for two independent variables was subjected to multiple regression to get quadratic polynomial equation:

Y_2 (full model) =+0.0358-0.0018X_1+0.0057X_2-0.0010X_1X_2-0.0062X_1^2-0.0007X_2^2

It is evident from the above equation that there are wide range of values for various coefficients. The X_2 and X_1^2 (P<0.05) were found to be significantly affecting response Y_2. The coefficient value for independent variable X_1 (-0.0018) showed the negative response on the dependent variable Y_2, i.e. on increasing carrier amount from 4 mg to 6 mg, it leads to increase in saturated solubility but further increasing from 6 mg to 8 mg, it decreases saturated solubility. The coefficient value for X_2 (0.0057) indicates the positive effect on response Y_2, i.e. on increasing adsorbate amount leads to marginal increase in saturated solubility. The terms X_2 and X_1^2 having P value < 0.05 were significant in contributing in estimation of particle size. The reduced equation for Y_2 can now be described as:

Y_2 (Reduced model) =+0.0358+0.0057X_2+0.0001X_1^2

Figure 7a shows 2D contour plot and 3b exhibits 3D response surface plot of saturated solubility. It is clearly observed from the graphs that the amount of carrier initially increases the saturated solubility up to 6 mg and then decreases while the amount of adsorbate increases saturated solubility also increases.

Overlay and Checkpoint Analysis

The overlay plot helped to obtain acceptable fields for the independent variables. The yellow area in the overlay plot exhibits the required design space within which the anticipated results for the responses can be obtained. The Figure 8 showed the favored ranges of the variables and their responses are as follows:

time required for 85% release (9.27 min) and saturated solubility (0.0395 mg/mL). Also, the design space provided a range for the factors: amount of carrier (4–8) and amount of adsorbate (0-3).

Optimization

The optimized batch was selected from an overlay plot of response variables and various solutions were analyzed. The formulation composition with amount of carrier and amount of adsorbate were observed to fulfil the required properties of an optimum formulation of immediate release parameter. The composition of optimized solid dispersion tablets is given in Table 8. The solid dispersion for the final formula was composed of 0.435 g of RXN, 6 g of PEG 4000 and 3 g of Neusilin US2.

Table 8
Formulation table of optimized batch of solid dispersion tablets

Ingredients	**Quantity (mg)**
Solid dispersion adsorbate	216
Crospovidone	15
Micro crystalline cellulose	64
Talc	2.5
Magnesium stearate	2.5
Total weight	**300 mg**

Evaluation of Optimized SDA

The optimized SDA of RXN was prepared and evaluated for flow property. The angle of repose of optimized formula was found to be 17.25±0.29^{o}, which show excellent flow, the Hausner's ratio was found to be 1.17±0.08, which show excellent flow and Carr's index was found to 9.20±0.65, which also depicts excellent flow property. Saturated solubility study was performed on SDA of RXN. The saturated solubility was found to be 0.041±0.0007 mg/mL in distilled water which was more than the pure drug because of the presence of Neusilin US2 in the batch which increased the surface area of the particles and hence the solubility of the formulation also enhanced. The drug content of optimized SDA was found to be 98.61%±1.18, which was in the acceptable range and confirms the integrity of the drug in the formulation. The optimized SDA of RXN was evaluated for percentage yield in the ratio obtained through overlay plot and was found to be 95.84±0.86%.

Evaluation of Optimized SDA Tablet

The optimized SDA tablet had been evaluated for its average weight (300±2.97 mg), thickness (3.44±0.01 mm), hardness (2.41 kg/cm^2), friability (0.32±0.02%) and disintegration time (26±2.64 sec). All the parameters were in the acceptable range. *In vitro* drug release profile of pure RXN, immediate release SDA tablet, marketed product and directly compressible tablet are shown in figure 9. From the *in vitro* release

patterns, it was clear that, optimized SDA tablet showed the fastest dissolution rate ($P < 0.0001$) as compared to other tested formulations. The optimized batch showed more than 85% dissolution in 10 min. The enhancement in the dissolution of RXN from SDA tablets can be due to several factors like enhanced drug surface area available for release, an improved wettability of the drug particles leading to an increased aqueous solubility of the drug.

Cell Viability Test

The cytotoxicity exhibited by the RXN SDA tablet and suspension containing RXN are shown in Figure 10. MTT assay was employed for cytotoxicity studies on Caco-2 cells. Cell viability of SDA tablet and suspension was evaluated at five different concentrations: 20 µM, 40 µM, 60 µM, 80 µM and 100 µM. Drug containing formulations exhibited a weak inverse correlation between concentration and cell viability. The highest concentration (100 µM) of RXN SDA tablet and RXN suspension exhibited a 95% cell viability indicating absence of cytotoxicity. RXN suspension exhibited similar cytotoxicity as that of RXN SDA, suggesting that the developed formulation did not precipitate any additional toxicity.

Pharmacokinetic Study

Based on the plasma concentration-time profiles, corresponding pharmacokinetic parameters were determined and tabulated in Table 9. The T_{max} for RXN SDA tablets was 2 h, whereas the value for RXN suspension was 3h. The rapid rate of absorption for RXN SDA tablets relative to RXN suspension could likely to provide a quick onset of action. This result can be attributed to the increase in dissolution rate and solubility of RXN from the SDA tablets in the gastrointestinal tract, allowing rapid absorption of the drug. The C_{max} values for RXN suspension, and RXN SDA tablets were found to be 262.32 ± 32.71 ng/mL, and 628.83 ± 42.60 ng/mL respectively. C_{max} values for RXN SDA tablets were 2.4 times more than RXN suspension indicating better release from formulation and consequent drug absorption in the systemic circulation. Mean AUC_{0-24} values achieved with RXN suspension, and RXN SDA tablets indicate significant ($P < 0.00001$) enhancement of bioavailability from RXN SDA tablets (Table 9). The overall relative bioavailability enhancement noticed with RXN SDA tablets was ~3 folds higher than the RXN suspension. Higher C_{max} and AUC achieved with test formulation indicated enhancement in oral bioavailability. The results of this study show a good correlation with the *in vitro* release studies. The outcomes of this study may be extrapolated towards the possibilities of dose reduction upon the administration of the test formulation. Similar observation was noticed in earlier studies with other drugs as well (49).

Table 9
Pharmacokinetic parameters for different rivaroxaban formulations after administration in Sprague-Dawley rats

Parameters	Rivaroxaban suspension	Rivaroxaban solid dispersion tablet
Tmax (h)	3.0	2.0
Cmax (ng/mL)	262.32 ± 32.71	628.83 ± 42.60
AUC_{0-24} (ng.h/mL)	1414.09 ± 192.18	3945.37 ± 300.71
$AUC_{0-\infty}$ (ng.h/mL)	1462.00 ± 207.35	4257.14 ± 311.15
Relative bioavailability	-	2.79 folds

Pharmacodynamic Studies

Tail Bleeding Time Assay

To discern the antithrombotic and associated antihemostatic effects of 0.5% CMC (control), RXN suspension, and RXN SDA tablets; bleeding time was investigated in the rat tail model. In the present study, bleeding time was markedly prolonged by all the formulations in comparison to control. The bleeding time noticed with RXN SDA tablets (189.00 ± 7.70s) was significantly higher ($P < 0.00001$) than RXN suspension (126.00 ± 6.52s) and vehicle (68.00 ± 9.08s). Overall, the data here demonstrated higher prolongation of bleeding time with RXN SDA tablets.

Platelet Aggregation

The effects of various formulations [0.5% CMC (control), RXN suspension, and RXN SDA tablets] on collagen induced platelet aggregation were evaluated 4 h post-dosing. Control group exhibited a value of 55.62 ± 2.95% whereas the values exhibited by RXN suspension and RXN SDA tablets were 24.37 ± 1.86%, and 13.78 ± 1.62%, respectively. The higher percentage of platelet aggregation noticed in RXN SDA tablets can be ascribed to the improved bioavailability of RXN, which ultimately increases the adenosine concentration and potentiates the antiplatelet action. The data are in agreement with previous pharmacodynamic studies (50) asserting the clinical benefit of the developed novel formulation of RXN.

Conclusion

This work demonstrated that SDA technique is a favorable approach for enhancing the bioavailability of drugs. The SDA mixture of drug carrier and adsorbent showed excellent flow properties and compressibility behavior and effortlessly compressed into tablets. Thus the compressing problems associated with conventional solid dispersion could be over counted. The optimized formula contains RXN, PEG 4000 as carrier, Neusilin US2 as an adsorbent in a molar ratio of 1:4:3. The optimized batch formulated as suggested by the experimental design showed higher drug dissolution rate as compared to pure RXN, immediate release SDA tablet, marketed product and directly compressible tablet. Also the

optimized formulation showed more than 85% dissolution in 10 min. Cytotoxicity indicates the safety, while pharmacokinetics and pharmacodynamics data substantiate the improvement in efficacy of RXN by the prepared SDA. Thus, SDA technique can be considered as a promising approach for the enhancement of bioavailability for poorly water soluble drugs like RXN.

Declarations

Ethics Approval and consent to participate: All institutional and national guidelines for the care and use of laboratory animals were followed.

Consent for publication: All authors have read and provided consent for the publication of the manuscript.

Availability of data and materials: All the data related to the manuscript has been included. The materials used in the experiments have been included in the material& methods section.

Funding: The funding for the research work was provided by Maliba Pharmacy College.

Competing interests: The authors have no conflict of interest.

Authors' contribution

Pranav J. Shah: Conceptualization, Data Curation, Formal Analysis, Investigation, Methodology, Writing—Review & Editing

Patel Milan Pankajkumar: Conceptualization, Data Curation, Formal Analysis, Investigation, Methodology, Writing—Original Draft Preparation

Jigar Shah: Formal Analysis, Investigation, Methodology, Writing—Review & Editing.

Sabna Kotta: Formal Analysis, Investigation, Methodology, Writing—Review & Editing. Anroop B Nair: Formal Analysis, Investigation, Methodology, Writing—Review & Editing.

Bhavin Vyas: Pharmacokinetic and pharmacodynamic studies, Writing—Review & Editing.

Acknowledgements: The authors acknowledge the management of Maliba Pharmacy College, Bardoli, Surat, India for the support.

Authors' information:

Pranav J. Shah is a Professor of Pharmaceutics at Maliba Pharmacy College, India.

Milan P. Patel is a post-graduate student at Maliba Pharmacy College, India.

Jigar Shah is a Professor of Pharmaceutics at Nirma University, India.

Anroop B. Nair is a Professor of Pharmaceutics at King Faisal University, Saudi Arabia.

Sabna Kotta is a Professor of Pharmaceutics at King Abdulaziz University, Saudi Arabia.

Bhavin Vyas is a Professor of Pharmacology at Maliba Pharmacy College, India.

References

1. Abouhussein DMN, Bahaa El Din Mahmoud D, Mohammad FE. Design of a liquid nano-sized drug delivery system with enhanced solubility of rivaroxaban for venous thromboembolism management in paediatric patients and emergency cases. Journal of liposome research. 2019;29(4):399–412. doi: 10.1080/08982104.2019.1576732.
2. Anwer MK, Mohammad M, Iqbal M, Ansari MN, Ezzeldin E, Fatima F, et al. Sustained release and enhanced oral bioavailability of rivaroxaban by PLGA nanoparticles with no food effect. Journal of thrombosis and thrombolysis. 2020;49(3):404–12. doi: 10.1007/s11239-019-02022-5.
3. Xue X, Cao M, Ren L, Qian Y, Chen G. Preparation and Optimization of Rivaroxaban by Self-Nanoemulsifying Drug Delivery System (SNEDDS) for Enhanced Oral Bioavailability and No Food Effect. AAPS PharmSciTech. 2018;19(4):1847–59. doi: 10.1208/s12249-018-0991-6.
4. Ding Z, Wang L, Xing Y, Zhao Y, Wang Z, Han J. Enhanced Oral Bioavailability of Celecoxib Nanocrystalline Solid Dispersion based on Wet Media Milling Technique: Formulation, Optimization and *In vitro*/ *In vivo* Evaluation. Pharmaceutics. 2019;11(7). doi: 10.3390/pharmaceutics11070328.
5. Zhang X, Xing H, Zhao Y, Ma Z. Pharmaceutical Dispersion Techniques for Dissolution and Bioavailability Enhancement of Poorly Water-Soluble Drugs. Pharmaceutics. 2018;10(3). doi: 10.3390/pharmaceutics10030074.
6. Sree Harsha N, Hiremath JG, Sarudkar S, Attimarad M, Al-Dhubiab B, Nair AB, et al. Spray dried amorphous form of simvastatin: Preparation and evaluation of the buccal tablet. Indian Journal of Pharmaceutical Education and Research. 2020;54:46–54.
7. Jacob S, Nair AB, Shah J. Emerging role of nanosuspensions in drug delivery systems. Biomaterials research. 2020;24(1):1–16.
8. Jacob S, Nair AB. Cyclodextrin complexes: Perspective from drug delivery and formulation. Drug development research. 2018;79(5):201–17. doi: 10.1002/ddr.21452.
9. Sherje AP, Jadhav M. β-Cyclodextrin-based inclusion complexes and nanocomposites of rivaroxaban for solubility enhancement. Journal of materials science Materials in medicine. 2018;29(12):186. doi: 10.1007/s10856-018-6194-6.
10. Chen N, Di P, Ning S, Jiang W, Jing Q, Ren G, et al. Modified rivaroxaban microparticles for solid state properties improvement based on drug-protein/polymer supramolecular interactions. Powder Technology. 2019;344:819–29. doi: https://doi.org/10.1016/j.powtec.2018.12.085.
11. Nepal PR, Han HK, Choi HK. Enhancement of solubility and dissolution of coenzyme Q10 using solid dispersion formulation. International journal of pharmaceutics. 2010;383(1-2):147–53. doi:

10.1016/j.ijpharm.2009.09.031.

12. Craig DQ. The mechanisms of drug release from solid dispersions in water-soluble polymers. International journal of pharmaceutics. 2002;231(2):131–44. doi: 10.1016/s0378-5173(01)00891-2.
13. Kapourani A, Eleftheriadou K, Kontogiannopoulos KN, Barmpalexis P. Evaluation of rivaroxaban amorphous solid dispersions physical stability via molecular mobility studies and molecular simulations. European journal of pharmaceutical sciences: official journal of the European Federation for Pharmaceutical Sciences. 2021;157:105642. doi: 10.1016/j.ejps.2020.105642.
14. Metre S, Mukesh S, Samal SK, Chand M, Sangamwar AT. Enhanced Biopharmaceutical Performance of Rivaroxaban through Polymeric Amorphous Solid Dispersion. Molecular pharmaceutics. 2018;15(2):652–68. doi: 10.1021/acs.molpharmaceut.7b01027.
15. Ganesh M. Design and optimization of rivaroxaban lipid solid dispersion for dissolution enhancement using statistical experimental design. Asian Journal of Pharmaceutics (AJP): Free full text articles from Asian J Pharm. 2016;10(1).
16. Alshehri S, Imam SS, Hussain A, Altamimi MA, Alruwaili NK, Alotaibi F, et al. Potential of solid dispersions to enhance solubility, bioavailability, and therapeutic efficacy of poorly water-soluble drugs: newer formulation techniques, current marketed scenario and patents. Drug delivery. 2020;27(1):1625–43. doi: 10.1080/10717544.2020.1846638.
17. Mahajan A, Surti N, Koladiya P. Solid dispersion adsorbate technique for improved dissolution and flow properties of lurasidone hydrochloride: characterization using 3(2) factorial design. Drug development and industrial pharmacy. 2018;44(3):463–71. doi: 10.1080/03639045.2017.1397687.
18. Kaushik D, Singh N, Arora A. Enhancement of dissolution profile of gliclazide by solid dispersion adsorbates. Lat Am J Pharm. 2011;30:2057–60.
19. Gupta MK, Goldman D, Bogner RH, Tseng YC. Enhanced drug dissolution and bulk properties of solid dispersions granulated with a surface adsorbent. Pharmaceutical development and technology. 2001;6(4):563–72. doi: 10.1081/pdt-120000294.
20. Hentzschel CM, Alnaief M, Smirnova I, Sakmann A, Leopold CS. Tableting properties of silica aerogel and other silicates. Drug development and industrial pharmacy. 2012;38(4):462–7. doi: 10.3109/03639045.2011.611806.
21. Wang Y, Zhao Q, Hu Y, Sun L, Bai L, Jiang T, et al. Ordered nanoporous silica as carriers for improved delivery of water insoluble drugs: a comparative study between three dimensional and two dimensional macroporous silica. International journal of nanomedicine. 2013;8:4015–31. doi: 10.2147/ijn.s52605.
22. Tawfeek HM, Roberts M, El Hamd MA, Abdellatif AAH, Younis MA. Glibenclamide Mini-tablets with an Enhanced Pharmacokinetic and Pharmacodynamic Performance. AAPS PharmSciTech. 2018;19(7):2948–60. doi: 10.1208/s12249-018-1108-y.
23. Nair AB, Chakraborty B, Murthy SN. Effect of polyethylene glycols on the trans-ungual delivery of terbinafine. Current drug delivery. 2010;7(5):407–14. doi: 10.2174/156720110793566308.

24. Shah J, Vasanti S, Anroop B, Vyas H. Enhancement of dissolution rate of valdecoxib by solid dispersions technique with PVP K 30 & PEG 4000: preparation and *in vitro* evaluation. Journal of Inclusion Phenomena and Macrocyclic Chemistry. 2009;63(1):69–75.
25. Altamimi MA, Elzayat EM, Qamar W, Alshehri SM, Sherif AY, Haq N, et al. Evaluation of the bioavailability of hydrocortisone when prepared as solid dispersion. Saudi pharmaceutical journal: SPJ : the official publication of the Saudi Pharmaceutical Society. 2019;27(5):629–36. doi: 10.1016/j.jsps.2019.03.004.
26. Farmoudeh A, Rezaeiroshan A, Abbaspour M, Nokhodchi A, Ebrahimnejad P. Solid Dispersion Pellets: An Efficient Pharmaceutical Approach to Enrich the Solubility and Dissolution Rate of Deferasirox. BioMed research international. 2020;2020:8583540. doi: 10.1155/2020/8583540.
27. Raval MK, Patel JM, Parikh RK, Sheth NR. Dissolution enhancement of chlorzoxazone using cogrinding technique. International journal of pharmaceutical investigation. 2015;5(4):247–58. doi: 10.4103/2230-973x.167689.
28. Jhaveri M, Nair AB, Shah J, Jacob S, Patel V, Mehta T. Improvement of oral bioavailability of carvedilol by liquisolid compact: optimization and pharmacokinetic study. Drug delivery and translational research. 2020;10(4):975–85. doi: 10.1007/s13346-020-00734-3.
29. Kwon J, Giri BR, Song ES, Bae J, Lee J, Kim DW. Spray-Dried Amorphous Solid Dispersions of Atorvastatin Calcium for Improved Supersaturation and Oral Bioavailability. Pharmaceutics. 2019;11(9). doi: 10.3390/pharmaceutics11090461.
30. Nair A, Gupta R, Vasanti S. *In vitro* controlled release of alfuzosin hydrochloride using HPMC-based matrix tablets and its comparison with marketed product. Pharmaceutical development and technology. 2007;12(6):621–5. doi: 10.1080/10837450701563277.
31. Harsha SN, Aldhubiab BE, Nair AB, Alhaider IA, Attimarad M, Venugopala KN, et al. Nanoparticle formulation by Büchi B-90 Nano Spray Dryer for oral mucoadhesion. Drug design, development and therapy. 2015;9:273–82. doi: 10.2147/dddt.S66654.
32. Nair AB, Al-Dhubiab BE, Shah J, Jacob S, Saraiya V, Attimarad M, et al. Mucoadhesive buccal film of almotriptan improved therapeutic delivery in rabbit model. Saudi pharmaceutical journal: SPJ : the official publication of the Saudi Pharmaceutical Society. 2020;28(2):201–9. doi: 10.1016/j.jsps.2019.11.022.
33. Nair AB, Sreeharsha N, Al-Dhubiab BE, Hiremath JG, Shinu P, Attimarad M, et al. HPMC- and PLGA-Based Nanoparticles for the Mucoadhesive Delivery of Sitagliptin: Optimization and *In vivo* Evaluation in Rats. Materials (Basel, Switzerland). 2019;12(24). doi: 10.3390/ma12244239.
34. Nair AB, Al-Dhubiab BE, Shah J, Attimarad M, Harsha S. Poly (lactic acid-co-glycolic acid) Nanospheres improved the oral delivery of candesartan cilexetil. Indian J Pharm Educ Res. 2017;51:571–9.
35. Sakure K, Kumari L, Badwaik H. Development and evaluation of solid dispersion based rapid disintegrating tablets of poorly water-soluble anti-diabetic drug. Journal of Drug Delivery Science and Technology. 2020;60:101942. doi: https://doi.org/10.1016/j.jddst.2020.101942.

36. Abdallah MA, Al-Ghobashy MA, Lotfy HM. Investigation of the profile and kinetics of degradation of rivaroxaban using HPLC, TLC-densitometry and LC/MS/MS: Application to pre-formulation studies. Bulletin of Faculty of Pharmacy, Cairo University. 2015;53(1):53–61. doi: https://doi.org/10.1016/j.bfopcu.2015.01.002.
37. Akrawi SH, Gorain B, Nair AB, Choudhury H, Pandey M, Shah JN, et al. Development and Optimization of Naringenin-Loaded Chitosan-Coated Nanoemulsion for Topical Therapy in Wound Healing. Pharmaceutics. 2020;12(9). doi: 10.3390/pharmaceutics12090893.
38. Chong J, Chen H, Dai D, Wang S, Zhou Q, Liu J, et al. Effects of ticagrelor on the pharmacokinetics of rivaroxaban in rats. Pharmaceutical biology. 2020;58(1):630–5. doi: 10.1080/13880209.2020.1785510.
39. Chaudhary S, Nair AB, Shah J, Gorain B, Jacob S, Shah H, et al. Enhanced Solubility and Bioavailability of Dolutegravir by Solid Dispersion Method: *In vitro* and *In vivo* Evaluation—a Potential Approach for HIV Therapy. AAPS PharmSciTech. 2021;22(3):127. doi: 10.1208/s12249-021-01995-y.
40. Nair A, Morsy MA, Jacob S. Dose translation between laboratory animals and human in preclinical and clinical phases of drug development. Drug development research. 2018;79(8):373–82. doi: 10.1002/ddr.21461.
41. Wang YY, Tang ZY, Dong M, Liu XY, Peng SQ. Inhibition of platelet aggregation by polyaspartoyl L-arginine and its mechanism. Acta pharmacologica Sinica. 2004;25(4):469–73.
42. Mekhfi H, El Haouari M, Legssyer A, Bnouham M, Aziz M, Atmani F, et al. Platelet anti-aggregant property of some Moroccan medicinal plants. Journal of ethnopharmacology. 2004;94(2-3):317–22. doi: 10.1016/j.jep.2004.06.005.
43. Born GV. Aggregation of blood platelets by adenosine diphosphate and its reversal. Nature. 1962;194:927–9. doi: 10.1038/194927b0.
44. Liu Y, Wang T, Ding W, Dong C, Wang X, Chen J, et al. Dissolution and oral bioavailability enhancement of praziquantel by solid dispersions. Drug delivery and translational research. 2018;8(3):580–90. doi: 10.1007/s13346-018-0487-7.
45. Vojinović T, Medarević D, Vranić E, Potpara Z, Krstić M, Djuriš J, et al. Development of ternary solid dispersions with hydrophilic polymer and surface adsorbent for improving dissolution rate of carbamazepine. Saudi pharmaceutical journal: SPJ : the official publication of the Saudi Pharmaceutical Society. 2018;26(5):725–32. doi: 10.1016/j.jsps.2018.02.017.
46. Sruti J, Patra Ch N, Swain SK, Beg S, Palatasingh HR, Dinda SC, et al. Improvement in Dissolution Rate of Cefuroxime Axetil by using Poloxamer 188 and Neusilin US2. Indian journal of pharmaceutical sciences. 2013;75(1):67–75. doi: 10.4103/0250-474x.113551.
47. Komínová P, Kulaviak L, Zámostný P. Stress-Dependent Particle Interactions of Magnesium Aluminometasilicates as Their Performance Factor in Powder Flow and Compaction Applications. Materials (Basel, Switzerland). 2021;14(4). doi: 10.3390/ma14040900.

48. Gupta MK, Tseng Y-C, Goldman D, Bogner RH. Hydrogen Bonding with Adsorbent During Storage Governs Drug Dissolution from Solid-Dispersion Granules. Pharmaceutical Research. 2002;19(11):1663–72. doi: 10.1023/A:1020905412654.
49. Kim SJ, Lee HK, Na YG, Bang KH, Lee HJ, Wang M, et al. A novel composition of ticagrelor by solid dispersion technique for increasing solubility and intestinal permeability. International journal of pharmaceutics. 2019;555:11–8. doi: 10.1016/j.ijpharm.2018.11.038.
50. Perzborn E, Heitmeier S, Laux V. Effects of Rivaroxaban on Platelet Activation and Platelet-Coagulation Pathway Interaction: *In vitro* and *In vivo* Studies. Journal of cardiovascular pharmacology and therapeutics. 2015;20(6):554-62. doi: 10.1177/1074248415578172.

Figures

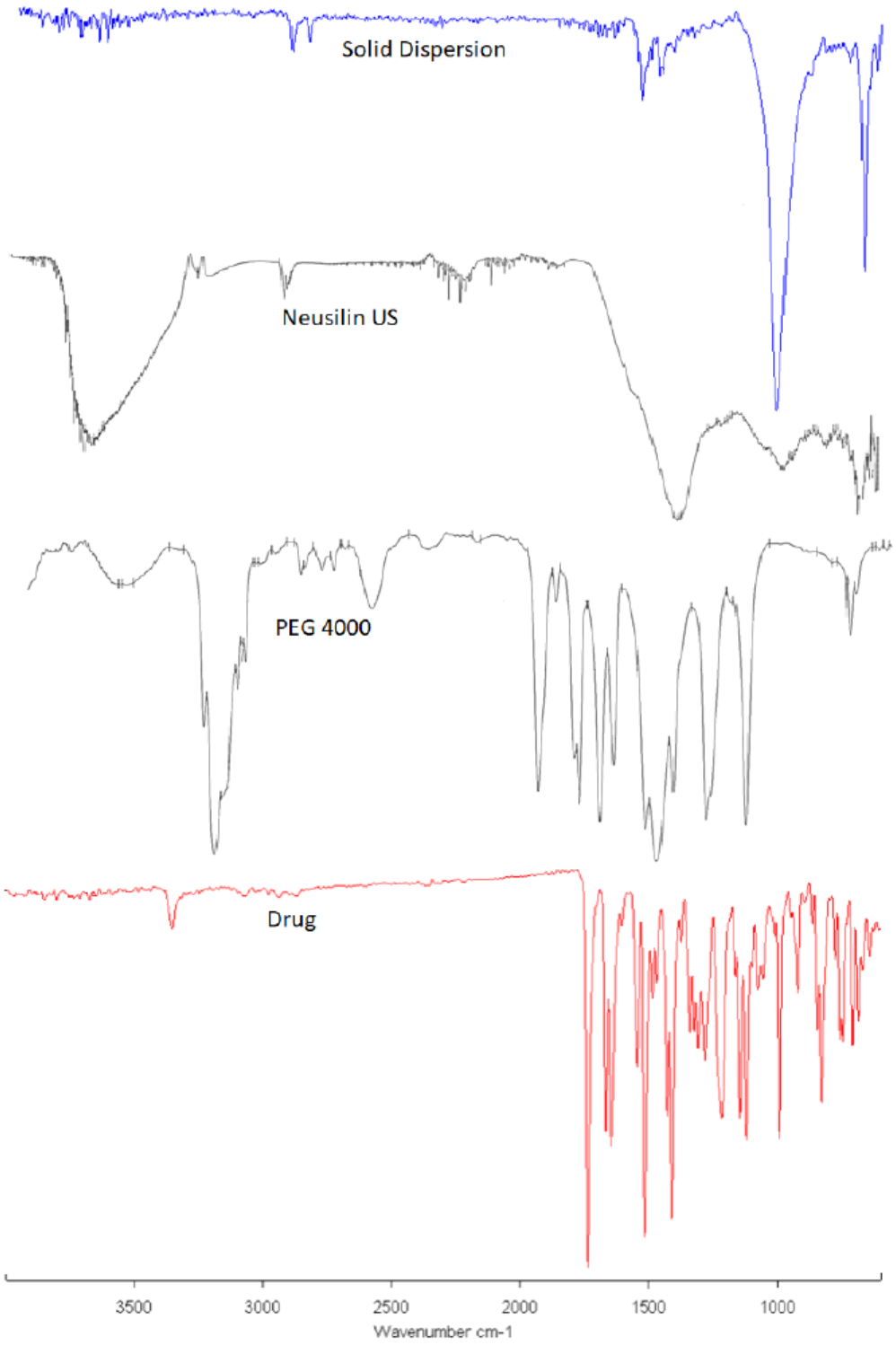

Figure 1

FTIR spectra of pure rivaroxaban, polyethylene glycol 4000, Neusilin US and solid dispersion adsorbate

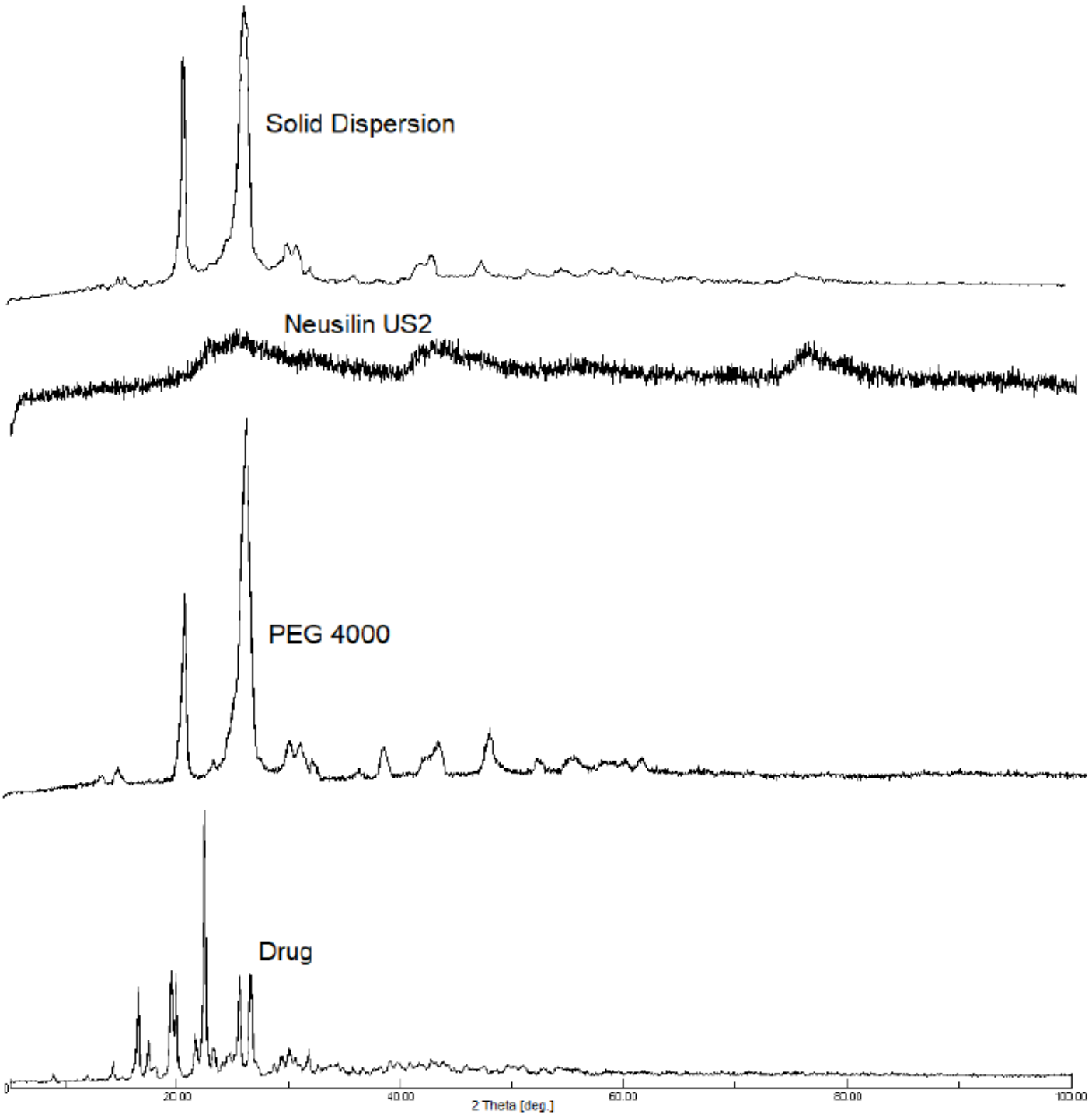

Figure 2

X-ray diffractogram of pure rivaroxaban, polyethylene glycol 4000, Neusilin US and solid dispersion adsorbate

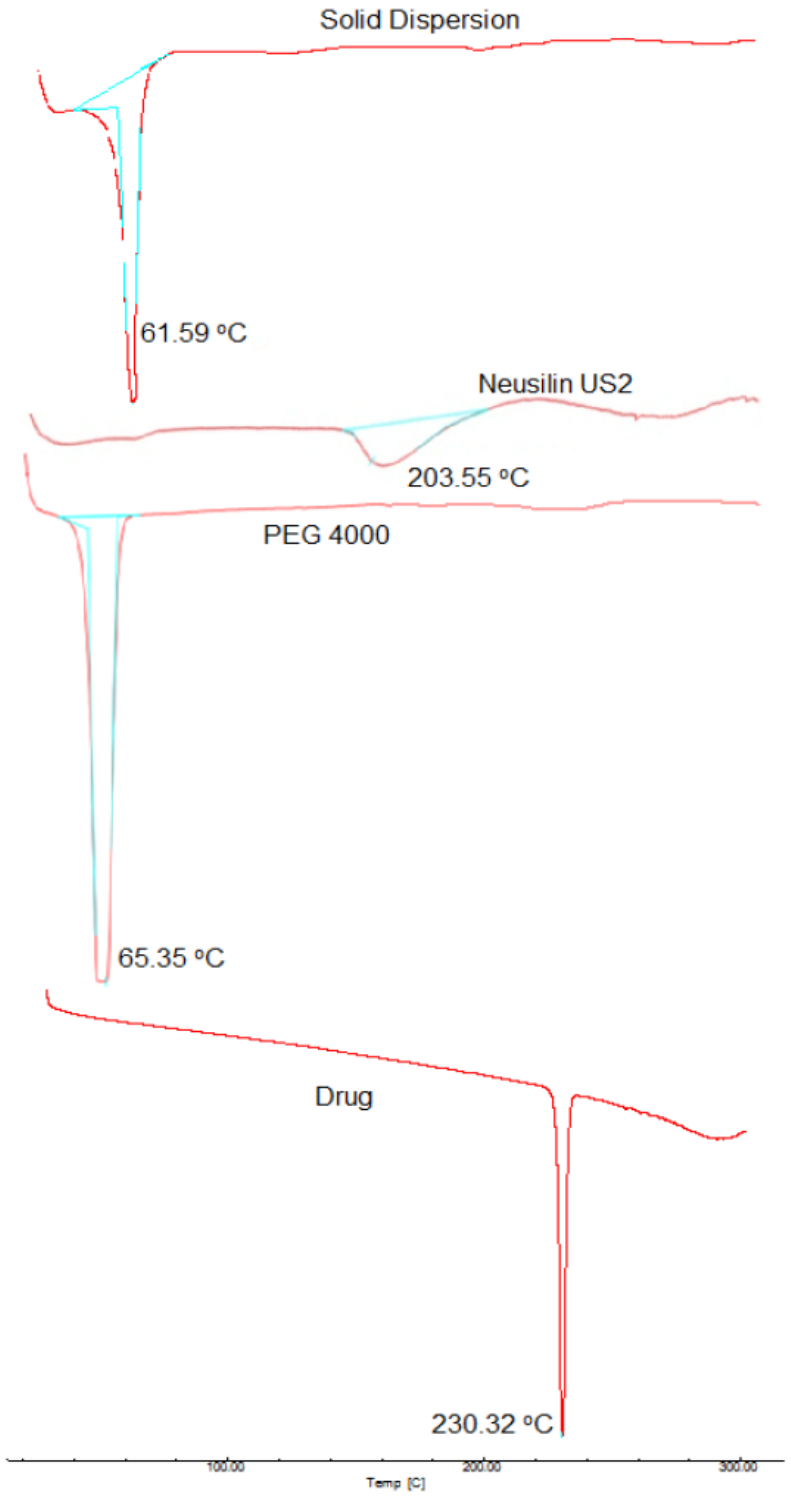

Figure 3

DSC thermograms of pure rivaroxaban, polyethylene glycol 4000, Neusilin US and solid dispersion adsorbate

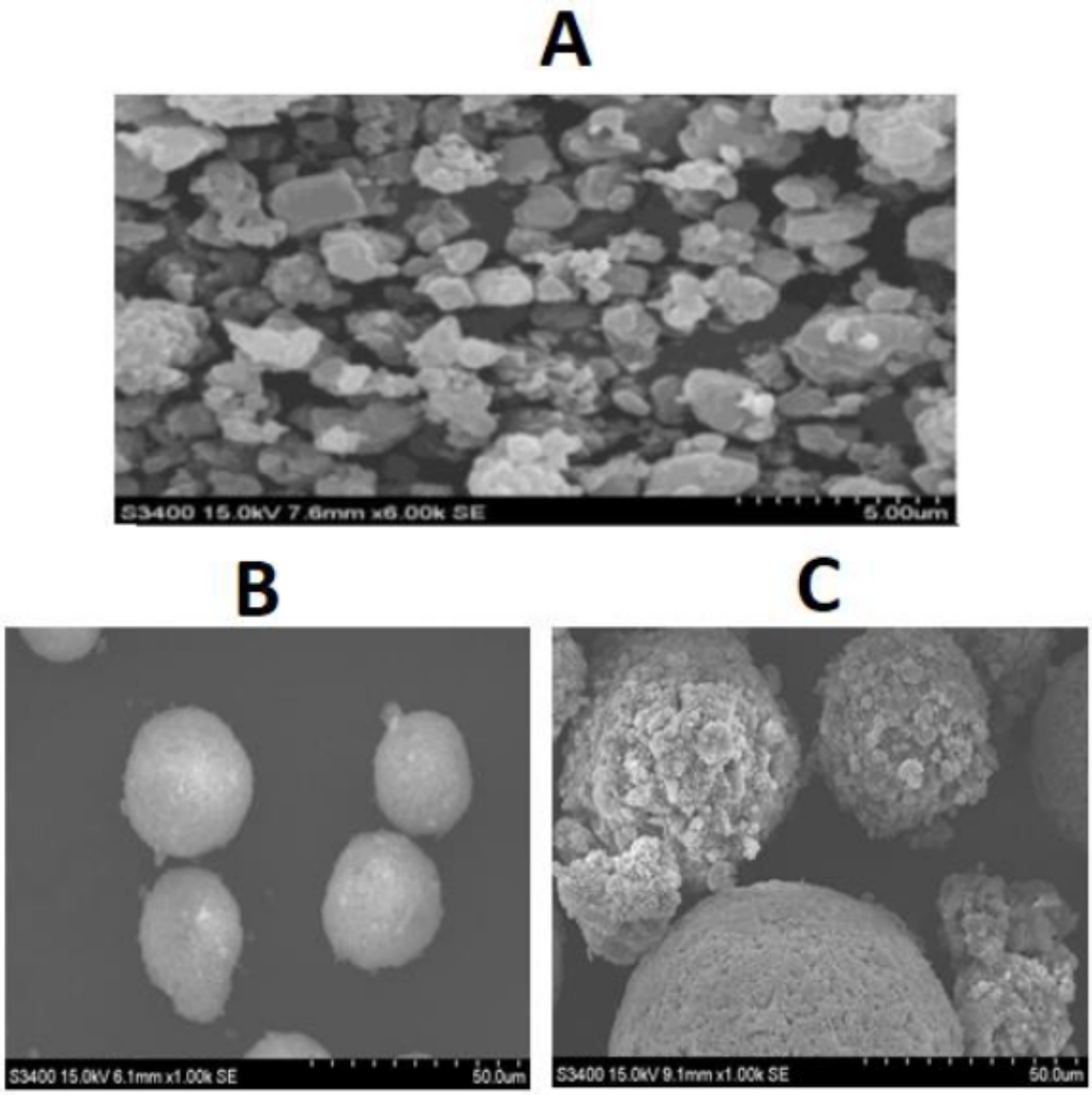

Figure 4

Scanning electron microscopy image of pure rivaroxaban (A), Neusilin US (B) and prepared solid dispersion adsorbate (C)

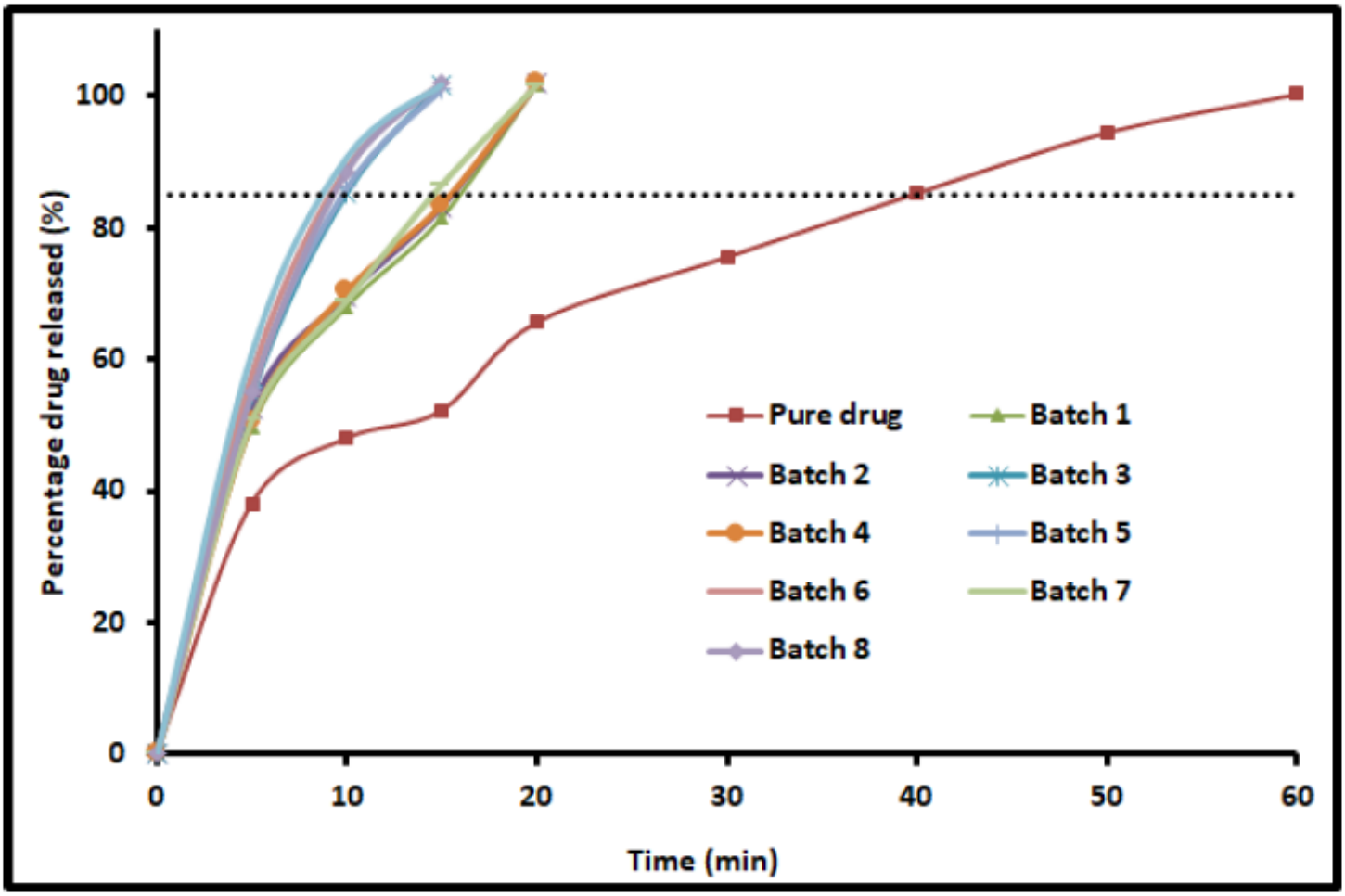

Figure 5

Comparison of in vitro dissolution profiles of rivaroxaban from immediate release solid dispersion adsorbate tablets and pure drug performed in a USP type II tablet dissolution test apparatus. Data presented as average of six trials ± SD

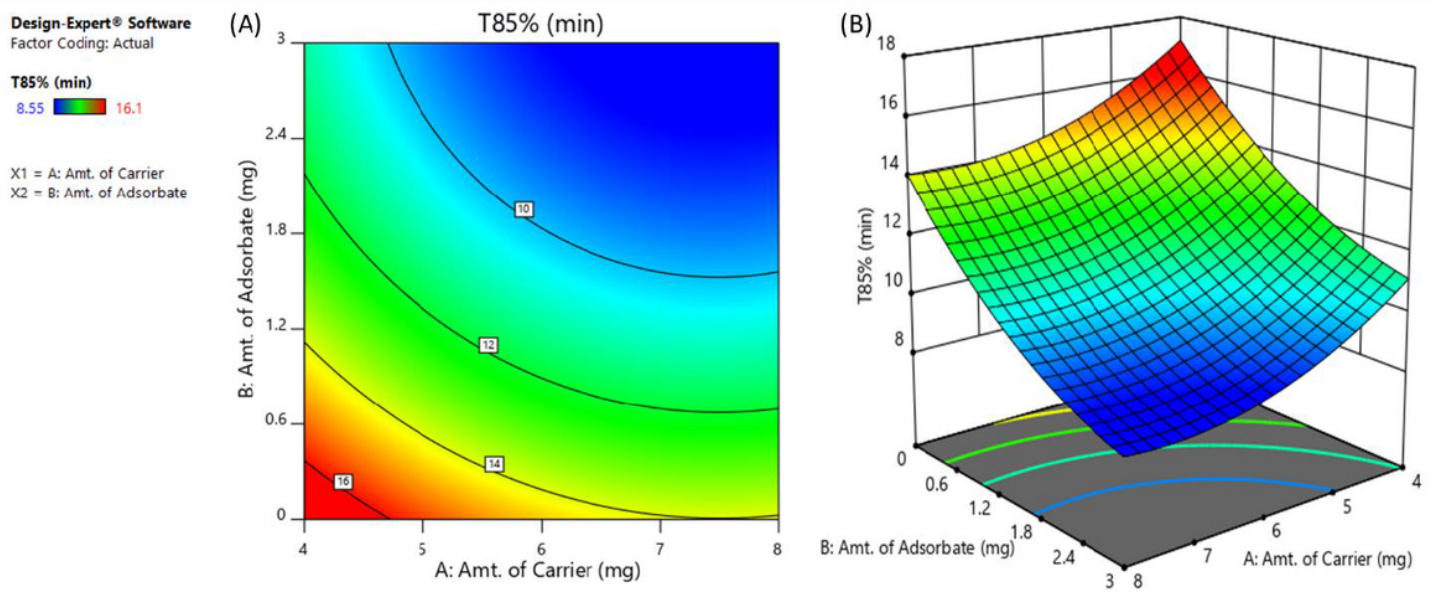

Figure 6

Contour plot (A) and 3D surface plot (B) showing the effect of amount of adsorbate and amount of carrier on time required for 85% drug release

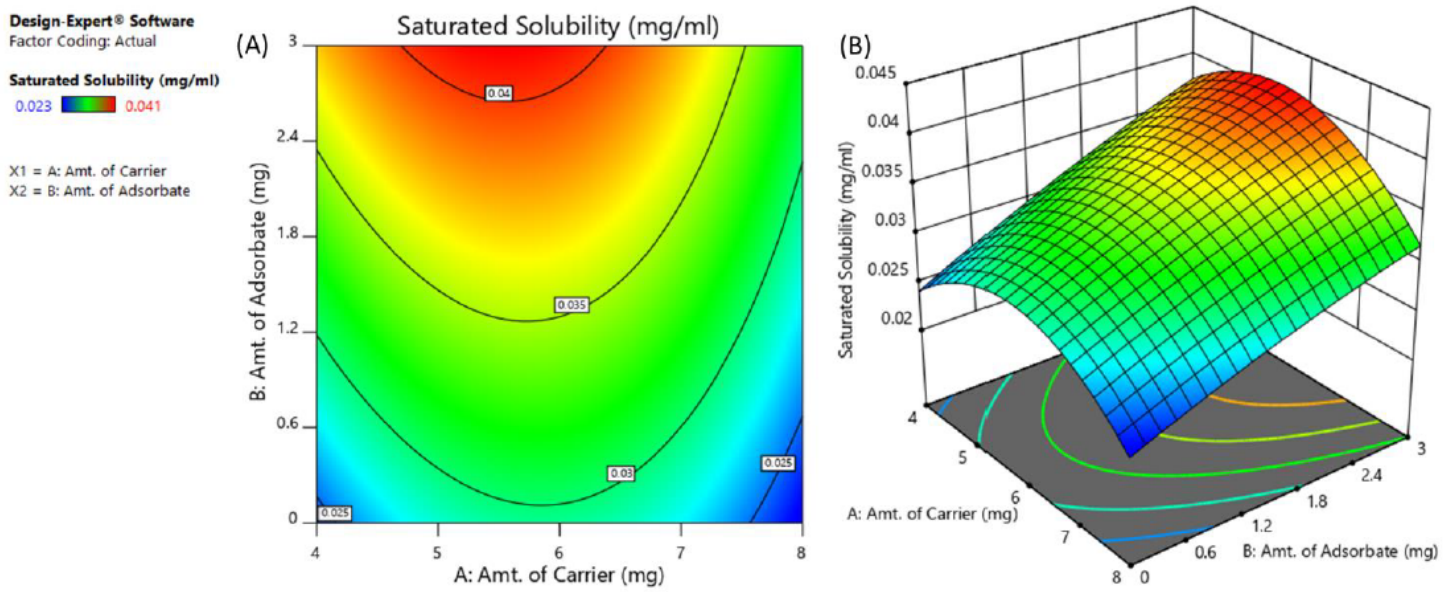

Figure 7

Contour plot (A) and 3D surface plot (B) showing the effect of amount of adsorbate and amount of carrier on saturated solubility

Design-Expert® Software
Factor Coding: Actual

Overlay Plot
T85%
Saturated Solubility

X1 = A: Amt. of Carrier
X2 = B: Amt. of Adsorbate

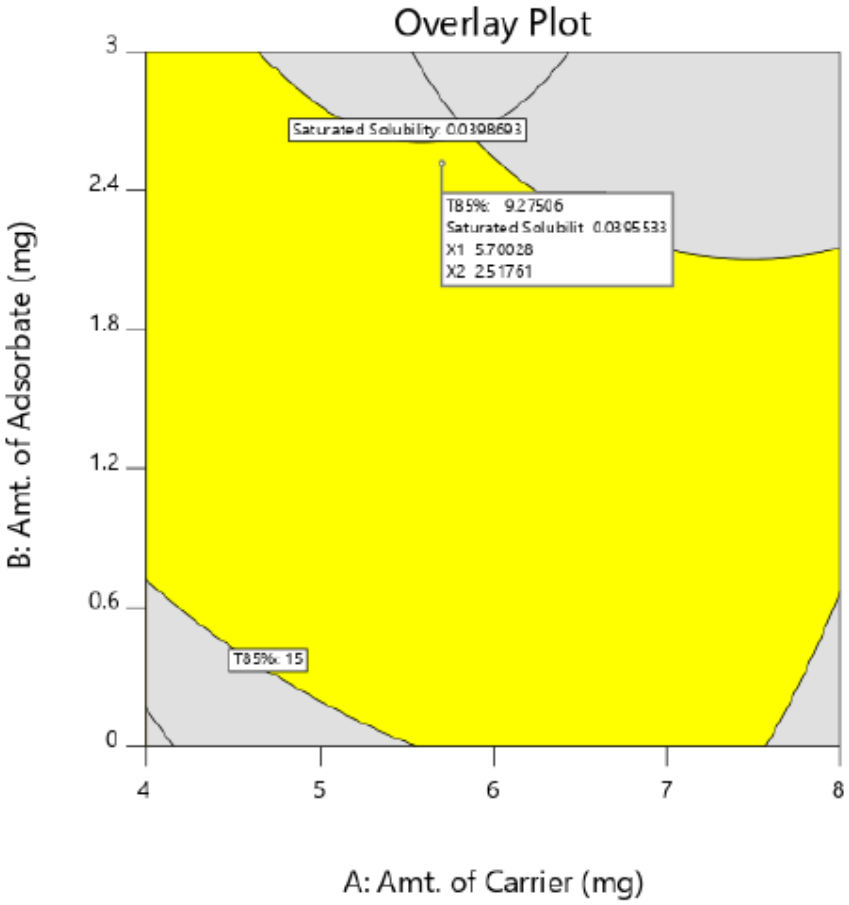

Figure 8

Overlay plot of the factors and responses

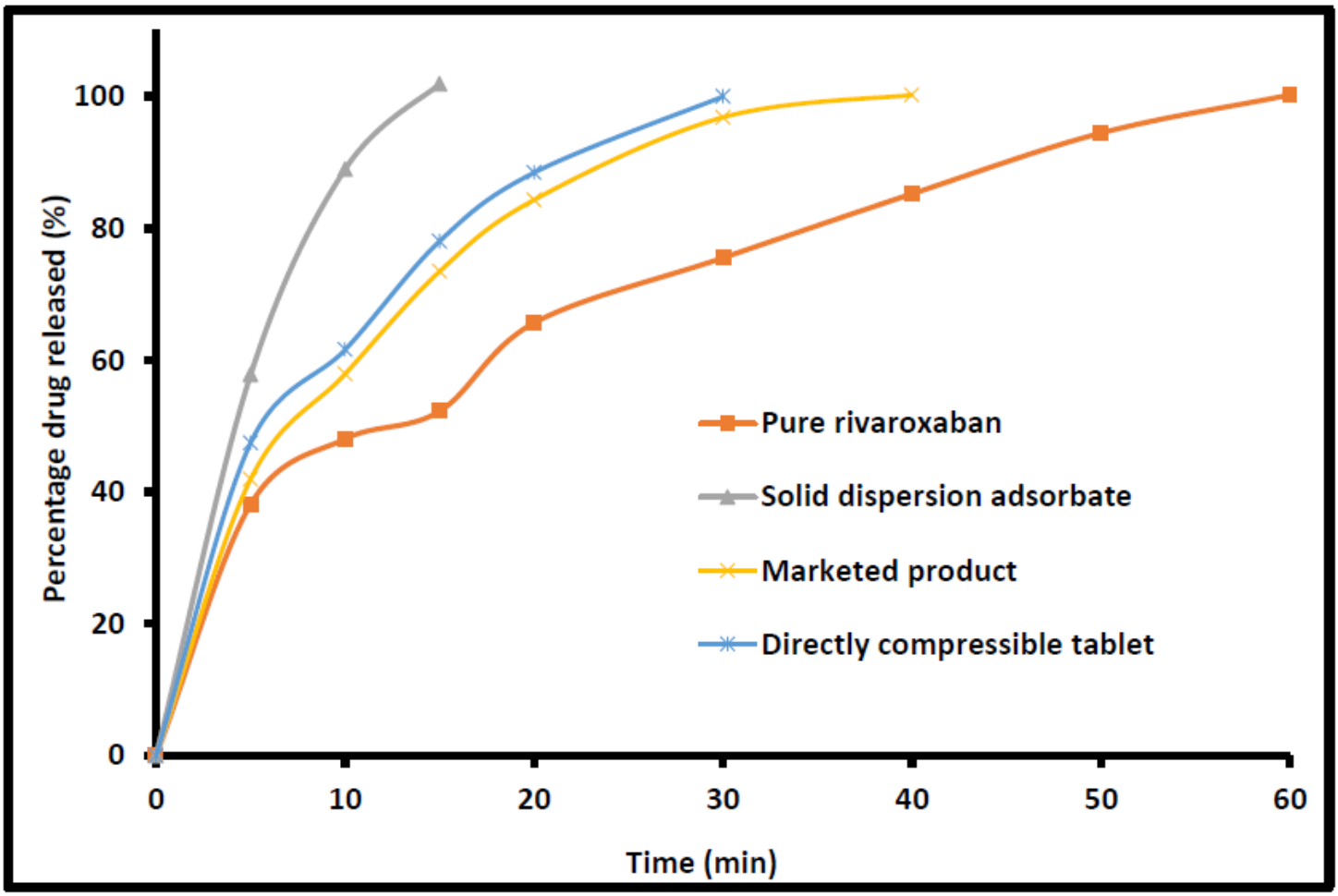

Figure 9

Comparison of in vitro dissolution profiles of pure rivaroxaban, immediate release solid dispersion adsorbate tablet, marketed product and directly compressible tablet performed in a USP type II tablet dissolution test apparatus. Data presented as average of six trials ± SD

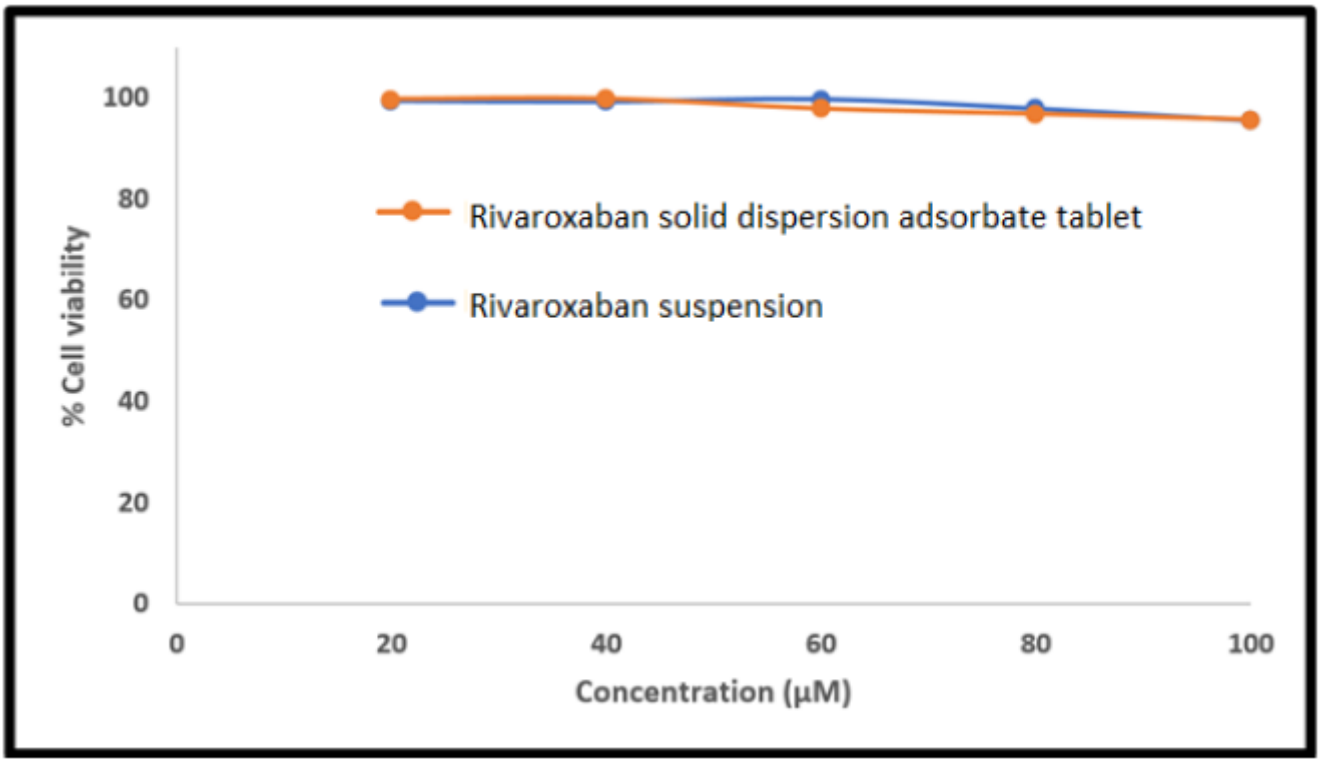

Figure 10

Results of cell viability analysis for the rivaroxaban solid dispersion adsorbate tablet and rivaroxaban suspension at various concentrations. Data presented as average of three trials ±

Supplementary Files

This is a list of supplementary files associated with this preprint. Click to download.

- GraphicalAbstarct.png